SORPTION OF TETRAVALENT THORIUM ON MUSCOVITE

M. Schmidt, S. S. Lee, R. E. Wilson, L. Soderholm[*], P. Fenter [1,*]

Chemical Sciences and Engineering Division, Argonne National Laboratory, Argonne, Illinois, 60439, USA

[*] *To whom correspondence should be addressed: fenter@anl.gov, ls@anl.gov*

ABSTRACT

Adsorption of tetravalent thorium to the (001) basal surface of phyllosilicate muscovite from an aqueous solution (1 x 10^{-4} mol/L Th(IV) in 1 x 10^{-1} mol/L NaCl, pH = 3.2) was studied by crystal truncation rod (CTR) and resonant anomalous x-ray reflectivity (RAXR) measurements. Th uptake to the muscovite surface from solutions with [Th] = 1 x 10^{-6} – 4.88 x 10^{-3} mol/L and 1 x 10^{-1} mol/L NaCl, pH = 3.2 was quantified by alpha-spectrometry. The uptake measurements showed that Th adsorption to the muscovite surface follows a Langmuir isotherm with an apparent adsorption constant K_{app} = 2 x 10^4 L/mol up to [Th] = 1.02 x 10^{-3} mol/L. The CTR and RAXR results identified one dominant Th species with a very broad distribution centered ~10 Å above the surface, in agreement with strongly hydrated extended outer sphere sorption. The findings indicate that the large energy of hydration (ΔG_{hyd} = -5815 kJ/mol (Marcus, 1991)) for the small and highly-charged Th^{4+} cation is a controlling parameter in its surface speciation. The surface occupancy (0.4 Th per unit cell area, A_{UC}) measured by RAXR exceeds the

expected level for surface charge compensation by tetravalent Th (0.25 Th/A_{UC}). However, the radiometric uptake measurements show smaller occupancies (0.21 Th/A_{UC}) after rinsing by deionized water, indicating a partial removability of sorbed thorium. Thorium oligomerization was observed at total Th concentrations $[Th]_{tot} \geq 2.0 \times 10^{-3}$ mol/L in presence of the surface, although solubility studies suggest that Th is soluble under these solution conditions.

1 INTRODUCTION

An early member of the 5f series, thorium is a primordial radioactive element that occurs naturally due to the long half-life of 1.41×10^{10} years of its most stable isotope ^{232}Th.

Because of its relatively simple solution chemistry (Wickleder et al., 2011) Th(IV) is often chosen as a chemical analog of the more radioactive, heavier members of the actinide series, notably Pu(IV). Such an approach is important especially in areas such as geochemistry because Th is a naturally occurring element whereas Pu is not. The analogy between Pu and Th is not, however, generally applicable and can itself further complicate attempts to understand Pu chemistry (Wilson, 2011). An understanding of Th chemistry for its own sake is useful to help delineate the similarities and differences in the behavior of these two elements. Toward this end, and to complement our efforts relevant to the understanding Pu migration in the environment (Fenter et al., 2010; Schmidt et al., 2012; Soderholm et al., 2008; Wilson et al., 2010), we report on experiments probing Th adsorption onto the (001) surface of muscovite mica.

Th exists in aqueous solution only as the tetravalent ion with a stable, $[Rn]^0$ electron configuration. It is the largest, chemically “softest”, and least polarizing of the tetravalent ions and as such is the least likely of these cations to undergo hydrolysis and subsequent

condensation reactions, both of which can significantly complicate the aqueous chemistry of higher-valent metal ions in general (Baes and Mesmer, 1976; Burgess, 1978). For example, these chemical attributes of thorium allowed for the isolation of the deca-aqua complex, $[Th(H_2O)_{10}]Br_4$ (Wilson et al., 2007a), to date the only reported homoleptic aqua compound of a tetravalent ion.

Despite its relatively simple aqueous chemistry, hydrolysis and subsequent oligomerization reactions significantly affect Th chemistry. These reactions and their products have been extensively studied in solution, with particular emphasis on the determination of thermodynamic stability constants for the hydrolysis products (Baes et al., 1958; Brown et al., 1983; Ekberg et al., 2000; Felmy et al., 1991; Knope et al., 2011; Neck et al., 2002; Rand et al., 2008; Ryan and Rai, 1987; Walther et al., 2008; Wilson et al., 2007b). Overall, it is clear that condensation of hydrolysed Th plays an important role in its solution chemistry, particularly with the observed presence of dissolved polynuclear species even at relatively low concentrations and acidic pH. Complementary solid-state studies provide insight into the stable structures of Th hydroxo-bridged dimers (Johansson, 1968; Wilson et al., 2007b), tetramers (Harrowfield et al., 1991), and hexamers (Knope et al., 2011; Takao et al., 2009). This chemistry must be considered when describing the sorption behavior of Th(IV) onto surfaces in contact with these solutions.

1.1 Thorium Sorption

Sorption of Th(IV) has been extensively studied on minerals and materials associated with host rock formations (Landa et al., 1995; Li and Tao, 2002; Östhols, 1995; Östhols et al., 1997; Zhang et al., 2006) and the geotechnical and technical barrier systems (Guo

et al., 2005; Jakobsson, 1999; Qian et al., 2010; Reiller et al., 2005; Rojo et al., 2009; Sharma et al., 2009; Sheng et al., 2008; Talip et al., 2009). The majority of these studies focused on quantifying thorium adsorption through the amount of Th(IV) removed from the solution, as determined by radiological or spectrophotometric methods, to derive a distribution coefficient K_d. However, this approach is limited by the fact that a thus derived coefficient will only be applicable for the circumstances under which it was measured. While most studies aim to provide coefficients for an array of solutions by varying ionic strength, pH, contact time, or the presence of additional ligands (PO_4^{3-}, fulvic and humic acids), K_d values do not lead to a more generalized understanding of thorium's sorption behavior on the molecular level.

Östhols and co-workers quantified the sorption of Th(IV) on amorphous silica in two studies: first using radiological methods and subsequently, complemented these results with extended x-ray absorption fine-structure (EXAFS) spectroscopy (Östhols, 1995; Östhols et al., 1997). The first study finds one "inner sphere" sorption species and a desorption process observed at high thorium concentrations ($[Th]_{tot} = 10^{-2}$ mol/L) that is attributed to the formation of thorium oligomers in solution by quantitative methods (Östhols, 1995). The subsequent EXAFS study on wet paste samples of various compositions (Östhols et al., 1997) confirmed the results. However, at the concentrations used in the Östhols study the formation of Th(IV)-(hydr)oxo-oligomers is expected (Walther et al., 2008) and Rothe et al. (Rothe et al., 2002) find clear indication for the formation of thorium oligomers in solution by EXAFS. The EXAFS signal measured by Östhols et al. is thus likely to represent a complex mixture of sorbed and dissolved mononuclear species, with sorbed or dissolved oligomers.

A different approach is taken by Degueldre and Kline (Degueldre and Kline, 2007) who model the sorption of Th(IV) on various colloidal mineral phases – Al_2O_3, TiO_2, FeOOH, and SiO_2 – using a simplified surface complexation model in consideration of hydrolysis and one-dimensional polymerization on the colloid surface. Based on the assumption that dissolved Th cations will preferentially adsorb on pre-adsorbed Th, the study suggests that the formation of surface bound polymers becomes the predominant interaction mechanism at thorium concentrations [Th] $>10^{-7}$mol/L. Our results suggest that a similar event may occur, however, only at significantly larger thorium concentrations [Th] > 10^{-3} mol/L.

1.2 X-ray Reflectivity

The complexity of the aqueous/mineral interface requires analytical techniques that are capable of probing the whole near-surface regime, while maintaining selectivity and sensitivity to different ion types and their speciation. X-ray reflectivity (XR) techniques – here referring to crystal truncation rod (CTR) measurements and resonant anomalous X-ray reflectivity (RAXR) – are capable of probing elemental distributions in near-surface regime, ranging in height from sub-monolayer adsorption structures to extended (few nm wide) distributions, with a high spatial resolution (i.e., <1 Å) in a single experiment. These techniques have been proven to be a versatile set of tools for probing complex geochemical systems (Fenter, 2002; Park et al., 2006; Park et al., 2005) and have proven particularly valuable when probing complex ion distributions (Catalano et al., 2008; Lee et al., 2010a; Lee et al., 2009). Detailed reviews on the methods can be found in the literature (Feidenhans'l, 1989; Fenter et al., 2007; Robinson and Tweet, 1992).

CTR measurements allow the structure of complex (buried) interfaces to be characterized by probing the electron density distribution near the interface. X-ray scattering from a two-dimensional interface results in one-dimensional "rods" of diffracted intensity in contrast to zero-dimensional Bragg "points" from a three-dimensional crystal. In the CTR experiment in a specular geometry, the rod intensity is measured as the ratio of the specularly reflected X-ray flux to the incident X-ray flux (i.e., R(q)) as a function of momentum transfer, $q = 4\pi/\lambda \sin(2\theta/2)$, where λ is the x-ray wavelength and 2θ is the scattering angle (i.e., the angle between incident and reflected x-rays).

These measurements are complemented by resonant anomalous X-ray reflectivity (RAXR), which adds elemental specificity to structures obtained from CTR experiments. RAXR experiments measure reflectivity as a function of incident photon energy near the absorption edge of the element of interest – here the Th L_{III} edge at 16.3keV – at fixed q. The spectra are fit first with a model-independent approach, followed by a model-dependent least-squares fitting which assumes a Th distribution at the interface (Park and Fenter, 2007).

In an initial effort to apply CTR/RAXR techniques to actinide sorption processes some of the potential complexities that may occur have been illustrated (Fenter et al., 2010). The sorption of trivalent plutonium on the muscovite (001) surface was investigated with ex-situ measurements (Fenter et al., 2010; Wilson et al., 2010). From a 10^{-3} mol/L Pu solution in a 10^{-1} mol/L $NaClO_4$ background electrolyte at pH = 3 Pu sorbed with a broad distribution at an average height of 18 Å, significantly larger than heights expected for any adsorbed inner- or outer-sphere complexes. The larger sorption height was interpreted to result from the adsorption of hydrated Pu maintaining multiple hydration

shells. The measured Pu coverage was also larger than the value expected for the surface charge compensation by trivalent Pu, and was interpreted to be indicative of an *in situ* oxidation of plutonium followed by formation of Pu-oxo-hydroxide clusters on the surface. In a second study, the sorption of Pu-oxo-nanoparticles at the muscovite (001) basal plane has been elucidated (Schmidt et al., 2012) revealing specifics of the nanoparticle-surface interaction. The nanoparticles were shown to adsorb on the (001) basal plane in one well-defined layer as well as in randomly distributed aggregates from an aqueous solution of monodisperse plutonium-oxide nanoparticles ($[Pu_{38}O_{56}Cl_x(H_2O)_y]^{(40-x)+}$, $[Pu]_{tot} = 10^{-3}$ mol/L, pH = 2.6). A large Pu surface loading of 10.8 Pu/A_{UC} was found, greatly exceeding the loading expected for Pu^{4+} adsorbed as mononuclear ions.

Here we present our results on the sorption of tetravalent thorium on the (001) basal plane of muscovite mica from 10^{-1} mol/L NaCl solution at pH = 3.2.

2 EXPERIMENTAL DETAILS

2.1 Materials

CAUTION! ^{230}Th is a radionuclide with a half-life of 7.54×10^4 years, ^{232}Th has a half-life of 1.41×10^{10} years. Both nuclides are alpha-emitters. The use of these nuclides requires the appropriate infrastructure and personnel trained in the handling of alpha-emitting isotopes.

2.1.1 Th(IV) solution

^{232}Th was chosen for CTR and RAXR measurements due to its very long half-life and reduced radiation hazards. Its low activity is not well-suited for the alpha-spectrometric

uptake measurements, especially for low surface loadings (e.g., $[Th]_{tot} = 10^{-6}$ mol/L). To increase the specific activity of the sorption samples, samples for the uptake measurements were exposed to increasing relative amounts of ^{230}Th ($t_{½}$ = 7.54 x 10^4 years) with decreasing total Th concentration $[Th]_{tot}$. A separate solution was prepared for each point on the uptake curve to have the desired pH. All solutions were prepared from Th stock solutions by dilution with solutions of appropriate concentrations of the background electrolyte and pH to avoid additional pH adjustments, which may lead to local supersaturation and precipitation events.

Summarized in Table 1 are details of the aqueous Th speciation in the solution used for the XR experiments, modeled based on data from the OECD-NEA thermodynamic database (Rand et al., 2008) and the NAGRA/PSI thermodynamic database (Hummel et al., 2002) with additions from other experimental data (Choppin and Jensen, 2011; Neck and Kim, 2001; Walther et al., 2008) using the PHREEQC solution modeling suite (version 2.17, (Parkhurst and Appelo, 1999)). The calculation is representative of the bulk solution. All solutions were prepared and equilibrated in air, with atmospheric CO_2 present. Dissolved carbonated species, e.g., CO_3^{2-}, were included in the calculations to reflect this.. The electrostatic attraction of the mica surface will lead to considerably altered concentrations in the solution in direct contact with the surface, which will also influence the speciation.

The modeling demonstrates that the Th^{4+} aqua ion is a minor species (13.9%) in the bulk at the relevant solution conditions. The hydrolysis product $ThOH^{3+}$ dominates the speciation (43.6%). The mono-chloro-complex ($ThCl^{3+}$: 30.7%) also contributes significantly to the thorium speciation. A mixed carbonate-hydroxo complex

($[Th(CO_3)_2(OH)_2^{2-}]$: 8.0%) and the second hydrolysis species ($[Th(OH)_2]^{2+}$: 3.5%) contribute to a lesser extent. The calculation does not indicate a significant presence of oligomers, with the dimer dominating such species at 0.19%. As a direct consequence of the hydrolysis and Cl^- complexation found by the PHREEQC calculation, the average charge of positively charged thorium species is reduced to +3.1 per Th from the nominal +4 charge. This is expected to increase the saturation sorption coverage of Th on muscovite which is driven by surface charge compensation, unless species of more highly-charged Th^{4+} adsorb preferably.

2.1.2 Muscovite substrates

Muscovite $KAl_2[AlSi_3O_{10}(OH,F)_2]$ is a phyllosilicate with a tetrahedral-octahedral-tetrahedral (TOT) layer structure, which is also a common building block of many clay minerals. The mineral exhibits perfect cleavage parallel to the (001) basal plane and has been frequently used as an analogue for clay minerals when high quality crystals or surfaces are required. The K^+ ions, which are located between the TOT layers in the bulk crystal structure, are exposed upon cleavage of the muscovite lattice and removed when the cleaved surface is immersed in water (Bowers et al., 2008; Cheng et al., 2001; Israelachvili and Wennerstrom, 1996; Lee et al., 2010a; Lee et al., 2010b; Park et al., 2006; Pashley, 1981, 1982; Schlegel et al., 2006). This leads to a fixed negative surface charge of $1e^-$ per area of the unit cell A_{UC} = 46.72 $Å^2$, corresponding to $0.021e^-/Å^2$. The surface charge is believed to be the main driving force behind cation sorption to the muscovite surface. In the presence of adsorbed cations a distinct layering of interfacial water on the surface was observed from surface force apparatus experiments and

interpreted as distinct hydration layers of the adsorbed cations (Israelachvili and Wennerstrom, 1996; Pashley, 1981, 1982).

The lattice spacing perpendicular to the (001) plane was found to be 19.95 ± 0.01 Å for this sample similar to the value from the literature (19.956 ± 0.003 Å) (Schlegel et al., 2006). V1 quality (clear, hard, of uniform color, nearly flat, free of all stains, foreign inclusion, cracks, and other similar defects) muscovite crystals (12.7 x 12.7 x 0.2 mm^3) from the Asheville-Schoonmaker Mica Company were used for all experiments. The (001) basal plane is nearly atomically flat and the geometrical crystal surface can be considered identical to the reactive surface, i.e. 161mm^2.

No significant interfacial roughness was observed by X-ray reflectivity, which is typical for muscovite in aqueous conditions (Cheng et al., 2001; Fenter et al., 2010; Lee et al., 2007; Schlegel et al., 2006). Dissolution of the muscovite substrate is expected to be negligible for the experiments (Lee et al., 2010a; Lee et al., 2009). Based on the dissolution rates published by Oelkers and coworkers (Oelkers et al., 2008) the expected release of Al^{3+} from a 12.7 x 12.7 mm^2 sample at pH = 3.2 over 2h will be below 10^{-11} moles. According to these calculations less than 0.001 monolayers of the substrate will dissolve within the duration of the experiment, in good agreement with the lack of observable interfacial roughness.

2.1.3 Sorption experiments

For alpha-spectrometry experiments muscovite crystals were cleaved to expose a fresh (001) surface and soaked in a solution of 10^{-1} mol/L NaCl at pH = 3.2 overnight. The samples were rinsed with deionized water (DIW), dried and submerged in the $^{230/232}$Th solutions with variable thorium concentrations and 10^{-1} mol/L NaCl as a background

electrolyte at pH = 3.2. A separate sample was used for every condition. After 2h of reaction the samples were removed from the Th(IV) solution, rinsed with ~2mL of deionized water and air-dried before alpha-counting. The air-drying is necessary for alpha-spectrometry to prevent absorption of alpha-particles in the supernatant solution. DIW was chosen to prevent the precipitation of NaCl upon air-drying.

For the X-ray reflectivity experiments freshly cleaved, and soaked samples were immersed in 2mL of a 1.1 x 10^{-4} mol/L ^{232}Th solution with 10^{-1} mol/L NaCl as background electrolyte at pH = 3.2 for 2h. The samples were removed from the ^{232}Th solution and promptly transferred to the sample cell pedestal (refer to the supporting information (S.I.) for detailed description on the sample cell). Twenty microliters of the Th(IV) solution were pipetted on the sample surface, which was then covered with a thin Kapton membrane (7.5 μm thick). The sample and the pedestal were then further enclosed in two independent layers of containment: (1) a 50 μm-thick Kapton dome and (2) a cylindrical Al cap with Kapton windows (75 μm thick). The cell was then transferred to the Advanced Photon Source (APS) where the X-ray reflectivity was measured.

2.2 Methods

2.2.1 Alpha spectrometry and uptake measurements

The method used for the alpha spectrometry was described in detail elsewhere (Wilson et al., 2010). Briefly, the dried samples were fixed on a steel planchette with epoxy and covered with a second planchette with a 33 mm^2 aperture. The second planchette masks all undesired radiation from the frayed edges of the muscovite crystal. An AlphaAnalyst

alpha-spectroscopy system from Canberra Inc. with a passivated implanted planar silicon (PIPS) detector (450 mm^2) and a 1024 channel multi-channel analyzer was used for the measurements. Energy calibrations were performed using a commercially prepared mixed alpha source standard of ^{238}U, ^{234}U, ^{239}Pu, and ^{241}Am (Analytics, Atlanta, GA, SS: 59949-121). The same source was used for count rate efficiency determinations.

The uptake curve was determined over the concentration range of [Th] = 1.0×10^{-6} – 4.9×10^{-3} mol/L, with relative amounts of ^{230}Th ranging from 1.7 to 100% (see Table 2). Samples were counted for 24h, resulting in statistical errors below 2.5%, with the exception at the lowest [Th] = 1.0×10^{-6}, where the statistical error is 6.3%.

2.2.2 CTR and RAXR measurements

All XR measurements were performed at the 6-ID-B undulator beamline (formerly μ-CAT) at the Advanced Photon Source (APS), with a beam size of ~0.05mm vertically and 1.0mm horizontally with a typical flux of $\sim 10^{12}$ photons/s. Specular reflectivity data were collected by reflecting the incident beam from the sample surface and detecting the reflected beam using an X-ray CCD detector (Fenter et al., 2006). For CTR measurements (i.e., non-resonant XR) the incident photon energy E was fixed at a value of 13.05keV, well below the Th L_{III} absorption edge (16.3keV). The reflected intensity was recorded as a function of momentum transfer in surface normal direction q. RAXR data were collected by scanning the energy through a 600eV range centered on the Th L_{III} edge at nine selected values of q. System stability for both measurements was ascertained by periodically returning to selected conditions and checking reproducibility.

The anomalous dispersion terms required for analyzing the RAXR data, as well as determining the exact absorption edge position of the studied Th sample under the given

conditions were derived from measuring fluorescence X-ray absorption near-edge structure (XANES) collected on the same sample in grazing-incidence mode using a Vortex^{TM}-brand Si-drift detector and applying a difference Kramers-Kronig transform (Cross et al., 1998; Fenter et al., 2010).

2.2.3 Data Analysis

The CTR measurement defines the total interfacial electron density, including that from water and adsorbed ions. CTR data were fit by applying a parameterized structural model consisting of the ideal muscovite substrate lattice and the interfacial region. The latter region included relaxation of the two top unit-cell layers of the muscovite surface, and the presence of near-surface species such as adsorbed species and water, as well as bulk water. The distribution of each adsorbed species is described as a Gaussian peak, whose structure factor is described as:

$$F = \sum_j c_j f_j(q) \exp\left(iqz_j\right) \exp\left[-\frac{q^2 u_j^2}{2}\right] \qquad (1)$$

where $f_j(q)$ is the atomic scattering factor and c_j, z_j, and u_j are the occupancy, height from the surface, and rms width of the jth atom. Bulk water was expressed by a layered water-model (Cheng et al., 2001; Schlegel et al., 2006). The quality-of-fit of each model was characterized by a scaled χ^2 and an R-factor (see S.I. for details).

The Th contribution to the electron density profile was determined by resonant anomalous x-ray reflectivity. RAXR analysis was achieved in two complementary steps: In the first step, semi-quantitative constraints on the elemental distribution were established (Fenter et al., 2007; Park and Fenter, 2007). The systematic variations in the resonant modulations' amplitude $A_R(q)$ and phase $\Phi_R(q)$ obtained from the model-

independent analysis of the RAXR spectra were used to estimate the surface loading θ of the resonant atom as well as an average height from the surface <z>. The actual variation of the amplitude and phase can be written as:

$$A_R(q)\exp[i\Phi_R(q)] = \sum_j c_j exp\left(-\frac{q^2u_j^2}{2}\right)\exp(iqz_j) \qquad (2)$$

where, c_j, u_j, and z_j are occupancy, rms width and average height of Th species j, respectively . A number of important constraints on the adsorption structure can be obtained from Eq. 2. The surface loading is estimated as $\Sigma_j(c_j) = \theta$ using the modulation amplitude in the limit of $q \rightarrow 0$, while the $q \rightarrow 0$ limit for $\Phi_R(q)/q$ corresponds to the average height of the elemental distribution (Park and Fenter, 2007). Additional information can be obtained from inspection of the q-dependence of the resonant amplitude and phase, such as the vertical width of the distribution and the relative heights of multiple distinct adsorption species, if any (Park and Fenter, 2007). The accuracy of this information is, amongst others, limited by the absence of data near q = 0. Nonetheless, this step is helpful in providing an unbiased initial model for the model-dependent RAXR fitting that defines the reported Th distribution.

The second step in the analysis is performed through a quantitative comparison of the RAXR data with a structural model composed of individual Gaussian peaks (Fenter et al., 2007). The resonant structure factor is expressed as

$$F_R(q) = (f'(E) + if''(E))\sum_j c_j \exp\left(iqz_j\right)\exp\left[-\frac{q^2u_j^2}{2}\right] \qquad (3)$$

Here f'(E) and f''(E) are the anomalous dispersion terms of the resonant element, in this case Th.

3 RESULTS

3.1 Uptake quantification

The data from the alpha-spectrometry experiment are shown in Figure 1 and summarized in Table 2. The interpretation of the results can be divided into two regimes. The low concentration range, [Th] $\leq 1.02 \times 10^{-3}$ mol/L, is adequately described by a Langmuir-type adsorption isotherm with an adsorption edge at 5×10^{-5} mol/L, corresponding to an apparent adsorption constant, $K_{app} = 2 \times 10^{4}$ L/mol. Langmuir-adsorption behavior has been observed previously for mononuclear ionic adsorption at the muscovite (001) basal plane (Fenter et al., 2010; Park et al., 2008).

The derived K_{app} is expected to be smaller than the intrinsic adsorption constant because of competition for sorption with Na^+ and hydronium. The intrinsic adsorption constant of Th was calculated using previously determined intrinsic adsorption constants for Na^+ and H_3O^+, (Park et al., 2008; Pashley, 1982) as

$$K_0 = K_{app} (1+c_{Na}K_{Na} + c_H K_H) \qquad (4)$$

where K_0 and K_{app} are intrinsic and apparent adsorption constants of Th, c_{Na} and c_H are concentrations of Na^+ and hydronium, and K_{Na} and K_H are the intrinsic adsorption constants of Na^+ and hydronium, respectively. The calculation yields an intrinsic adsorption constant $\log K_0$ (Th(IV)) = 6.6 ± 0.2. The intrinsic adsorption constant for Th(IV) is smaller than that for Pu(III) under similar solution conditions ($\log K_0$ (Pu(III)) = 7.8 in 10^{-1} mol/L $NaClO_4$ at pH = 3 (Fenter et al., 2010)) but larger than the values observed for Rb^+ and Sr^{2+} ($\log K_0$ (Rb^+) = 4.1, $\log K_0$ (Sr^{2+}) = 5.7 (Park et al., 2008)). These results suggest that the intrinsic adsorption strength of Th(IV) is larger than that of the mono- and divalent cations, respectively, but smaller than that of the trivalent

plutonium ion. Following the trend of increasing adsorption strength with increasing metal-ion valence established for Rb^{+}, Sr^{2+} and Pu^{3+}, it was expected that the tetravalent cation would exhibit stronger interaction with the negatively charged muscovite surface than the other three, assuming the reaction is solely electrostatically driven. The deviation from the expected trend for the more highly charged ions may be related to differences in the hydration free energy between Pu^{3+} and Th^{4+} (-3235kJ/mol and -5815kJ/mol, respectively (Marcus, 1991)). The closer approach of more strongly hydrated Th^{4+} to the muscovite surface (i.e., transition of Th^{4+} from the diffuse layer to the Stern layer) exacts a greater dehydration-energy cost than it does for Pu^{3+} (Lee et al., 2010a). However, direct comparison between these two results is limited because of the different background electrolyte system, which may influence the interfacial speciation beyond the simple competition by Na^{+} or H_3O^{+}, and differences in the hydrolysis behavior of Pu^{3+} and Th^{4+}. Alternatively, the results may reflect the average charge of the adsorbed species, which we estimate to be +2.4 based on the intrinsic adsorption constant of Th compared with a trend from those measured for divalent Sr^{2+} and trivalent Pu^{3+}. This would indicate the adsorption of multiple hydrolyzed mononuclear $Th(OH)_n^{(4-n)+}$ species and/or their condensation products or possibly $ThCl_n^{(4-n)+}$ complexes.

At concentrations up to [Th] = 1.02 x 10^{-3} mol/L the Langmuir isotherm yields a maximum coverage for ionic Th^{4+} adsorption of (0.21 ± 0.02) Th/A_{UC} (Figure 1), reasonably close to the expected surface loading needed for surface charge compensation by a tetravalent ion (0.25 M^{4+}/A_{UC}). The samples exposed to higher Th(IV) concentrations ([Th] ≥ 1.97 x 10^{-3} mol/L), however, show surface loadings that are greater than the expected maximum surface loading. At the highest solution concentration

[Th] = 4.88 x 10^{-3} mol/L we find a surface loading of more than 2 Th/A_{UC}. Obviously, these results cannot be explained by a Langmuir-type adsorption process of simple cations, but instead imply the occurrence of a surface induced precipitation event. It is not clear which phase precipitates and if it is a crystalline or colloidal ("amorphous") phase. In the absence of the muscovite surface, all solutions are stable and no solid Th phases are supersaturated. Among these undersaturated phases, "amorphous" $Th(OH)_4$ has the highest saturation index, but is still well undersaturated with a saturation index S.I. = -0.63. No attempt was made to characterize the phase because the amounts of precipitates were very small ($\leq 10^{-9}$ mol; Table 2).

3.2 Interfacial Structure

The measured specular reflectivity is presented (in Figure 2a) in the range of q = 0.2 – 5.3 $Å^{-1}$ (corresponding to L = 0.6 – 16.8 reciprocal lattice units). The data shows typical large variations in reflectivity over several orders of magnitude of dynamic range. The calculated reflectivity based on the best-fit model is shown as blue line. The electron density profile derived from the best-fit model is shown in Figure 3 as a black line. It features two pronounced peaks at 2.1 Å and 3.9 Å from the surface, two smaller peaks at 5.2 Å and 6.8 Å and a broad distribution extending out to ~20 Å. The model reproduces the data (χ^2 = 6.9, R = 5.6%). CTR experiments probe the whole interfacial structure, and consequently we cannot uniquely distinguish the Th(IV) electron density from that of other constituents of the adsorption structure: Na^+, Cl^- and water.

The specific contribution of Th(IV) to the structure was determined by RAXR. Representative RAXR spectra are shown in Figure 2b. The data show strong modulations at low q that decrease quickly with increasing q. Both the resonant amplitude and the

phase variations with q, derived from the model-independent analysis (Park et al. 2007), change systematically as a function of q, as shown in Figure 4. From this analysis we determine a surface loading of 0.4 Th(IV)/A_{UC} and an average height of 10 Å.

This information is used to develop the element-specific, vertical electron density distribution of adsorbed Th, which is shown in Figure 3 (blue area). The thorium distribution extends approximately 20 Å from the surface, with a maximum density at 10.1 Å. The distribution is slightly asymmetric with a higher density closer to the surface. The model reproduces the measured RAXR spectra (χ^2 = 1.3, R = 0.7%), as well as the amplitude and phase behavior shown in Figure 4.

A number of different models and starting conditions have been employed in attempting to fit the data. These models, however achieved a quality of fit poorer than the reported model. It appears noteworthy that the data cannot be reproduced by a simple diffuse profile as would result from an electrical double layer as described by the Gouy-Chapman model (Bourg and Sposito, 2011; Chapman, 1913). Models describing the exponential decay expected in a diffuse layer fail to reproduce the measured RAXR spectra, and, moreover, exhibit an amplitude variation as a function of q that does not match the observed behavior. Full details of the electron density models, those reported in the manuscript as well as less successful models, can be found in the supplementary information.

4 DISCUSSION AND CONCLUSIONS

The major species in the Th(IV) adsorption structure at the muscovite (001)-aqueous solution interface is broadly distributed, with a center at 10.1 Å. This height is too large to be simply attributed to classical inner- or outer-sphere species adsorbed directly on the

surface. The observed electron density can be understood when it is compared with previous studies on the adsorption of hydrated cations on the muscovite (001) basal plane. Similar adsorption heights were observed previously for strongly hydrated divalent cations (e.g., Pb^{2+} or Hg^{2+}) and were interpreted as the height of an extended outer sphere complex, i.e. adsorption of cation with two hydration shells intact (Lee et al., 2010a). Occurrence of this species has been attributed to a large hydration free energy. In the case of most divalent cations, this species occurred as a minor constituent of the whole adsorption structure which co-existed with inner- or outer-sphere species (Lee et al., 2010a). Its occurrence as the dominant form of interaction between cation and surface in the thorium system can be understood when we take into consideration that the small and highly-charged Th(IV) ion has a hydration free energy (ΔG_{hyd} = -5815 kJ/mol (Marcus, 1991)) that is substantially larger than that of any divalent cation (cp. ΔG_{hyd} (Be^{2+})= -2395 kJ/mol, largest of the divalent cations (Marcus, 1991)). In fact, the charge density in Th(IV) is sufficiently large to maintain two strongly-bound hydration layers (David and Vokhmin, 2003).

The final best fit model for the RAXR data consists of two Gaussians at 7.6 ± 0.2 and 10.3 ± 0.5Å, respectively. The first is a minor component with a total occupancy of 0.04 Th/A_{UC} with the majority of Th concentrated in the second peak with an occupancy of 0.39 Th/A_{UC}. However, both peaks are broad (2.01 and 4.65Å, respectively) and overlap to form a continuous electron density profile, which is shown in Figure 3. Based on the available data we cannot distinguish whether the two peaks represent two distinct species, or rather one asymmetrical distribution.

The presented results shed light on the sorption of tetravalent thorium on the muscovite (001) basal plane from a 10^{-1} mol/L NaCl aqueous solution at pH = 3.2. The uptake measurements show two concentration regimes in which different interaction modes prevail.

At low thorium concentrations [Th] = 1.0 x 10^{-6} – 1.0 x10^{-3} mol/L we observe Langmuir-type adsorption, with an intrinsic adsorption constant of logK_0 = 6.6 ± 0.2 and a maximum surface loading of θ(Th) = (0.21 ± 0.02) Th/A_{UC}. However, the RAXR analysis yields a larger surface loading of θ(Th) = 0.4 Th/A_{UC} albeit the data were measured at [Th] = 1.0 x 10^{-4} mol/L (i.e., at the concentration slightly above the adsorption edge (5 x 10^{-5} mol/L)). The surface loading measured by RAXR is considerably larger than the surface loading (θ(Th) = 0.15 Th/A_{UC}) measured by alpha-spectrometry under the solution condition used for the CTR/RAXR measurements (Table 2). This difference can be explained by noting that the muscovite sample was rinsed with DIW and dried in air before the alpha-spectrometry measurement. The reduced coverage obtained with alpha-spectrometry therefore indicates adsorbed Th can be partially removed during rinsing. It is unclear from the available data whether the surface loading found by alpha-spectrometry is controlled by a slow desorption rate of Th in DIW (during the rinsing step) or the difference in the adsorption strengths between multiple thorium species at the interface. It could be speculated that there are minor species of inner or outer sphere adsorbed Th that are less readily removed from the surface if they form a stronger bond with the surface ligands than the extended OS complex. However, the electron density of Th within the typical adsorption height range for inner- and outer-sphere species (~1.5 – 5 Å) accounts for ~15% of the total coverage (or 0.06 Th/A_{UC})

measured by RAXR, significantly less than the thorium coverage (0.15 Th/A_{UC}) measured by alpha-spectrometry.

The surface loading obtained by RAXR also exceeds the value expected based on charge compensation considerations. This may be partly explained by the average charge of Th species in the solution being lower than +4 due to hydrolysis and complexation by Cl^- (Table 1). Adsorption of cations on the muscovite (001) surface is an electrostatically driven process, and consequently the more highly-charged aqua ion is expected to adsorb preferentially. The amount of $Th^{4+}(aq)$ in the solution exceeds the amount needed to fully compensate the muscovite surface charge by a factor of 30. Moreover, the maximum surface loading derived from the Langmuir isotherm matches the expected value for Th^{4+} (0.25 Th^{4+}/A_{UC}), suggesting that the dominant sorption species is the Th^{4+} aqua ion. However, the concentration of the trivalent species (i.e., $ThOH^{3+}$ and $ThCl^{3+}$) is about ~5 times larger than that of the aqua ion, which should promote their adsorption. A conclusive decision on the surface speciation would require a specific sorption constant for $Th^{4+}(aq)$ separately from those for $ThOH^{3+}$, and $ThCl^{3+}$, but these values are not currently available. The increased surface loading may also be due to the high charge on Th ions that leads to large distances between adsorbed ions. This leads in turn to local charge imbalances, since the surface charge is evenly distributed across the surface. This may also be the reason the observed surface loading is even larger than the expected value, based on the average charge of Th species in solution. It can be expected that this nominal over-compensation of the muscovite charge by Th will be accompanied by the co-adsorption of anion species, likely Cl^- for the current solution conditions.

The thorium-specific electron density profile is broad, distributed over more than 20 Å and without sharp features. As mentioned above, this width may be partly related to the interfacial speciation of thorium and thus include minor contributions from inner and outer sphere complexes. The distribution is, however, nearly symmetrical and less hydrated Th species cannot explain electron density at larger distance from the muscovite surface. It is thus reasonable to assume that the width of the distribution is predominantly related to an intrinsic vertical mobility of the extended outer sphere Th complex. The vertical distribution may also be related to fluctuations in the hydration shell of an adsorbed species or slight differences in the hydration shells of chemically different adsorbed species (e.g. the hydration shell of Th^{4+} will differ from that of $ThCl^{3+}$).

The second concentration regime at [Th] $\geq 2.0 \times 10^{-3}$ mol/L exhibits enhanced thorium-surface loading up to a value of θ(Th) = 2.1 Th/A_{UC} at [Th] = 4.9×10^{-3} mol/L. No saturation in the coverage was observed at elevated concentrations. It seems unlikely that this behavior can be explained by mononuclear, ionic adsorption because the surface loading is significantly greater than that needed for compensation of the surface charge. The enhanced uptake rather may result from oligomer formation or a precipitation event. The observed surface loading value is lower than the value observed for the sorption of pre-formed $[Pu_{38}O_{56}]^{40+}$-nanoparticles on muscovite (10.8 Pu/A_{UC}) (Schmidt et al., 2012). It is noteworthy that even the solution with the highest Th concentration [Th] = 4.9×10^{-3} mol/L is expected to be stable with respect to precipitation while it contains ~20% Th-(hydr)oxo-oligomers (Neck et al., 2002; Walther et al., 2008). Consequently, the observed precipitation event appears to be induced by adsorption to the muscovite surface.

The presented results reveal the interaction mechanism of tetravalent thorium with the muscovite (001) basal plane. In the low concentration regime the interaction is dominated by mononuclear extended-outer-sphere sorption of strongly-hydrated Th(IV). This adsorbed species was shown to be at least partly removable by rinsing with DIW, which may be related to thorium's high vertical mobility, as demonstrated by RAXR. The higher surface loadings related to surface induced precipitation, however, increase the uptake capacity of muscovite relative to the maximum coverage for charge compensation by nearly a factor of ten. These results are expected to have implications far beyond the studied system, in particular for other mineral phases structurally related to muscovite as well as other tetravalent actinides. Clay minerals are naturally abundant and also under consideration as active components of engineered barriers at nuclear waste disposal sites, in the USA (DePaolo, 2007), France (Gaucher et al., 2004), and Switzerland (Pearson et al., 2003). These minerals share many structural features with the investigated muscovite, and we expect similar interfacial reactivity on the corresponding interfaces. Moreover, other actinides, most notably plutonium are also predominantly tetravalent and thus may behave in a manner similar to tetravalent Th. The results will also add to previous studies regarding the sorption behavior of cations of different valence at the muscovite/aqueous interface (Lee et al., 2010a; Park et al., 2008; Pashley and Israelachvili, 1984; Sakuma and Katsuyuki, 2011; Schlegel et al., 2006).

Acknowledgments. This work conducted at Argonne National Laboratory, operated by UChicagoArgonne LLC for the United States Department of Energy under contract number DE-AC02-06CH11357, is jointly supported by the United States Department of Energy Office of Science, BER, NSF, and the EPA. The X-ray reflectivity data were

collected at the X-ray Operations and Research beamline 6-ID-B at the Advanced Photon Source (APS), Argonne National Laboratory. Additional XR measurements were performed at beamline 13-ID-C, GSECARS, at the APS.

Supporting Information Available. Details on the CTR and RAXR data analyses, and on the thin film cell used in the XR experiments.

TABLES

Table 1: Calculated solution speciation. $[Th]_{tot}$ = 1.0 x 10^{-4} mol/L, 1 x 10^{-1} mol/L NaCl, pH = 3.2.

Species	Conc. [mol/L]	%
$ThOH^{3+}$	4.4 x10^{-5}	43.6
$ThCl^{3+}$	3.1 x10^{-5}	30.7
Th^{4+}	1.4 x10^{-5}	13.9
$Th(CO_3)_2(OH)_2^{2-}$	8.0 x10^{-6}	8.0
$Th(OH)_2^{2+}$	3.5 x10^{-6}	3.5
$Th_2(OH)_3^{5+}$	1.9 x10^{-7}	0.4
$Th(OH)_3^{+}$	3.8 x10^{-8}	0.0
$Th_2(OH)_2^{6+}$	1.5 x10^{-8}	0.0
$Th(OH)_4^{0}$ (aq)	1.7 x10^{-11}	0.0
	1.0 x10^{-4}	100.0

%: percentage of total Th present in this chemical form

Table 2: Results of the uptake measurement.

[Th] (mol/L)	[^{230}Th] (%)	m(Th) (ng/cm^2)	n(Th) (nmol/cm^2)	θ(Th)/A_{UC}
4.88 x 10^{-3}	2.72	171.0	0.74	2.074
3.87 x 10^{-3}	1.72	66.9	0.29	0.812
2.92 x 10^{-3}	2.28	31.9	0.14	0.387
1.97 x 10^{-3}	3.38	25.6	0.11	0.310
1.02 x 10^{-3}	6.53	17.5	0.08	0.213
1.14 x 10^{-4}	13.06	13.6	0.06	0.165
1.00 x 10^{-4}	100.00	12.2	0.17	0.149
8.00 x 10^{-5}	100.00	11.7	0.05	0.143
5.00 x 10^{-5}	100.00	10.3	0.05	0.127
2.00 x 10^{-5}	100.00	5.8	0.04	0.070
1.00 x 10^{-5}	100.00	5.5	0.03	0.067
5.00 x 10^{-6}	100.00	4.1	0.02	0.050
1.00 x 10^{-6}	100.00	0.1	0.02	0.001

FIGURES

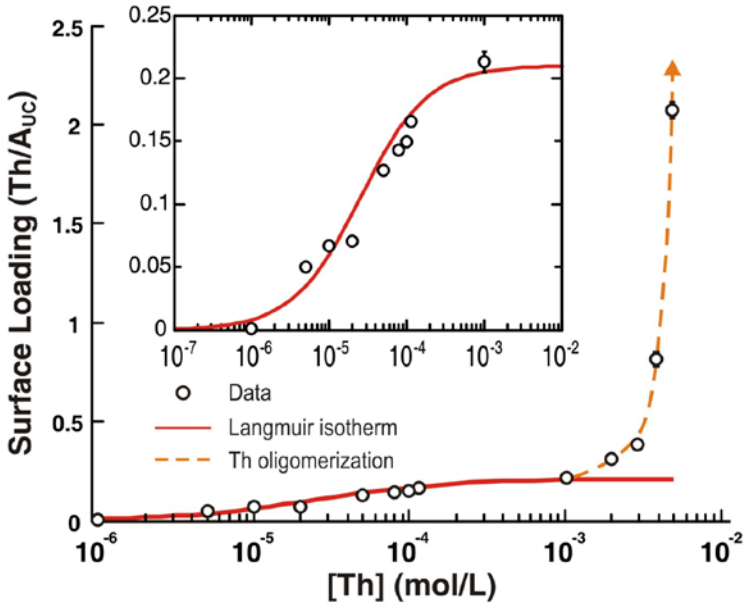

Figure 1: Th(IV) uptake measurement. Surface loading (in units of Th/A_{UC}) measured by alpha-spectrometry are plotted as a function of solution concentration in the Th concentration range [Th] = 1.0 x 10^{-6} – 4.9 x 10^{-3} mol/L. The best-fit Langmuir isotherm for the low concentration range is shown in a red solid curve. The orange dashed curve shows a trend representing excess uptake of Th by the surface-induced oligomerization. The inset shows the low concentration range [Th] = 1.0 x 10^{-6} – 1.0 x 10^{-3} mol/L that was used for the Langmuir isotherm fit (the labels for the axes of the inset plot are the same as that of the main figure. These data are also shown with a linear concentration scale in the supplementary information).

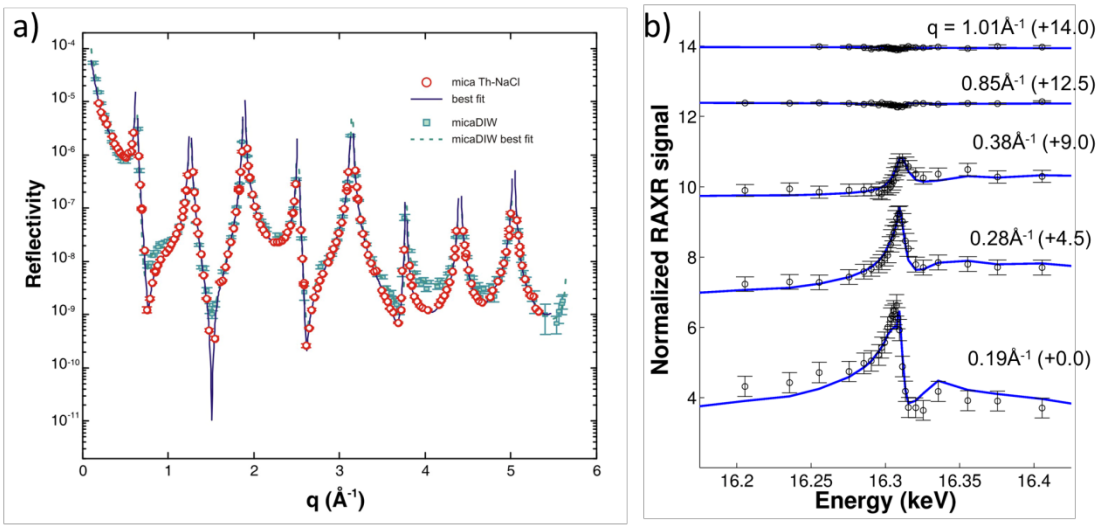

Figure 2: a) Specular X-ray reflectivity of the muscovite crystal (equilibrated with a solution of 1 x 10^{-4} mol/L Th(IV) at pH 3.2 with 1 x 10^{-1} mol/L NaCl background electrolyte) as a function of momentum transfer, q, measured with a photon energy E = 13.05 keV. Measured reflectivity data are shown (red symbols). The best fit is shown as thick blue line. The CTR data of muscovite (001) in deionized water (DIW) (Cheng et al., 2001) is shown for comparison (dashed green line and squares). b) Selected resonant anomalous X-ray reflectivity data (black circles) measured from the muscovite (001) surface equilibrated with the same solution. Five of a total of nine scans are shown. Each spectrum probes the variation of the specular reflectivity measured as a function of photon energy, E, at a different fixed momentum transfer, q (Å^{-1}), as indicated. Spectra are normalized using the resonance amplitude normalization $[(|F_{tot}(q,E)|^2 - |F_{NR}(q)|^2)/(2|F_{NR}(q)|)$, where F_{tot} and F_{NR} are total and non-resonant structure factors, respectively] and offset vertically for clarity (offset given in parentheses for each spectrum). The blue lines show the calculated intensities from the best-fit model.

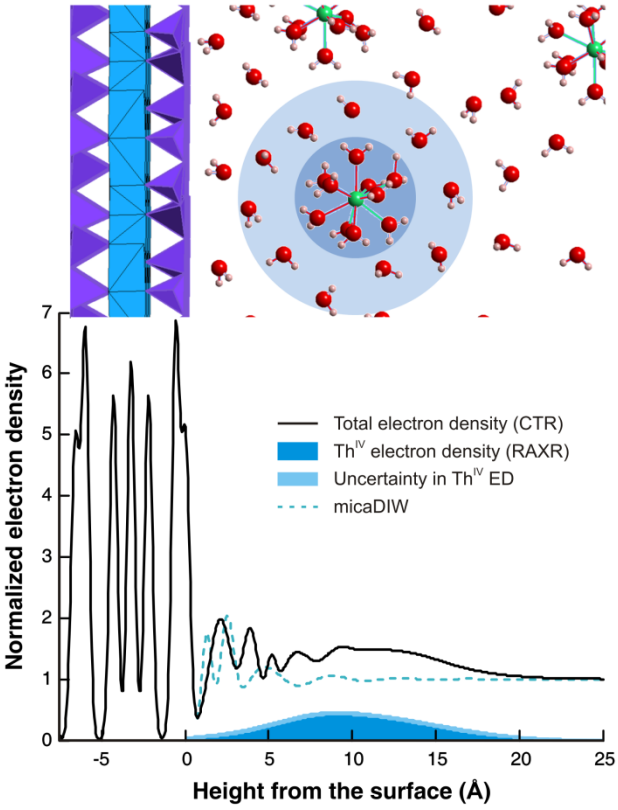

Figure 3: Interfacial Structure. Total electron density profile derived from CTR (Figure **2**a, black line) and Th electron density distribution derived from RAXR (Figure 2b, blue area, uncertainty in electron density (ED) in lighter blue). The ED profile measured at the muscovite – DIW interface (Cheng et al., 2001) is also plotted (dashed green line) for comparison. The electron density is normalized to that of bulk water ρ(bulk water) = $0.33e^{-}/Å^{3}$, so that the normalized ED of water is 1.00. The average height of muscovite surface oxygens is set to be z = 0Å. For illustration purposes a schematic representation of species contributing to the observed ED is shown in the upper part of the figure (Key: Purple tetrahedra: SiO_4, blue octahedra AlO_6, red spheres: O, white: H, green: Th). The shaded areas highlight the first and second hydration shells of Th(IV).

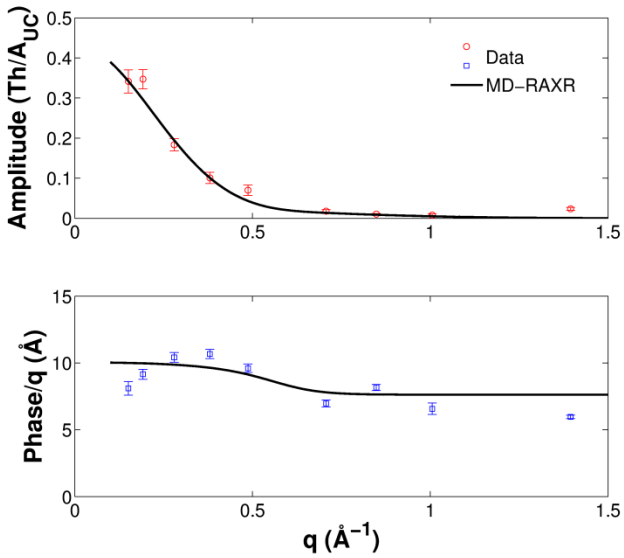

Figure 4: Amplitude and Phase variation. Amplitude and phase of the element-specific partial structure factors of Th(IV) adsorbed at muscovite (001)–aqueous solution interface determined by model-independent (data points) and model-dependent (solid lines) analyses of RAXR spectra.

REFERENCES

Baes, C.F., Bjerrum, J., Schwarzenbach, G., Sillen, L.G., 1958. Part II, Inorganic Ligands, Stability Constants. The Chemical Society, London, p. 6.

Baes, C.F., Mesmer, R.E., 1976. The hydrolysis of cations. John Wiley & Sons Inc., New Jersey.

Bourg, I.C., Sposito, G., (2011) Molecular dynamics simulations of the electrical double layer on smectite surfaces contacting concentrated mixed electrolyte ($NaCl–CaCl_2$) solutions. *Journal of Colloid and Interface Science* **360**, 701-715.

Bowers, G.M., Bish, D.L., Kirkpatrick, R.J., (2008) Cation Exchange at the Mineral−Water Interface: H3O+/K+ Competition at the Surface of Nano-Muscovite. *Langmuir* **24**, 10240-10244.

Brown, P.L., Ellis, J., Sylva, R.N., (1983) The hydrolysis of metal-ions. 5. Thorium(IV). *J. Chem. Soc. Dalton Trans.* **1983**, 31-34.

Burgess, J., 1978. Metal ions in solution. Ellis Horwood Ltd., Chichester, U.K.

Catalano, J.G., Park, C., Fenter, P., Zhang, Z., (2008) Simultaneous inner- and outer-sphere arsenate adsorption on corundum and hematite. *Geochim. Cosmochim. Acta* **72**, 1986-2004.

Chapman, D.L., (1913) LI. A contribution to the theory of electrocapillarity. *Philosophical Magazine Series 6* **25**, 475-481.

Cheng, L., Fenter, P., Nagy, K.L., Schlegel, M.L., Sturchio, N.C., (2001) Molecular-Scale Density Oscillations in Water Adjacent to a Mica Surface. *Physical Review Letters* **87**, 156103.

Choppin, G.R., Jensen, M.P., 2011. Actinides in Solution: Complexation and Kinetics, in: Morss, L.R., Edelstein, N.M., Fuger, J., Katz, J.J. (Eds.), The Chemistry of the Actinide and Transactinide Elements, 4th ed. Springer, pp. 2524-2621.

Cross, J.O., Newville, M., Rehr, J.J., Sorensen, L.B., Bouldin, C.E., Watson, G., Gouder, T., Lander, G.H., Bell, M.I., (1998) Inclusion of local structure effects in theoretical x-ray resonant scattering amplitudes using ab initio x-ray-absorption spectra calculations. *Physical Review B* **58**, 11215.

David, F.H., Vokhmin, V., (2003) Thermodynamic properties of some tri- and tetravalent actinide aquo ions. *New Journal of Chemistry* **27**, 1627-1632.

Degueldre, C., Kline, A., (2007) Study of thorium association and surface precipitation on colloids. *Earth. Planet. Sci. Lett.* **264**, 104-113.

DePaolo, D.J., 2007. Basic Research Needs for Geosciences: Facilitating 21st Century Energy Systems. U.S. Department of Energy, Office of Basic Energy Sciences, Bethesda, MD.

Ekberg, C., Albinsson, Y., Comarmond, M.J., Brown, P.L., (2000) Studies on the complexation behavior of thorium(IV). 1. Hydrolysis equilibria. *J. Sol. Chem.* **29**, 63-86.

Feidenhans'l, R., (1989) Surface-Structure Determination by X-Ray-Diffraction. *Surf. Sci. Rep.* **10**, 105-188.

Felmy, A.R., Rai, D., Mason, M.J., (1991) The solubility of hydrous thorium(IV) oxide in chloride media: development of an aqueous ion-interaction model. *Radiochim. Acta* **55**, 177-185.

Fenter, P., (2002) X-ray Reflectivity as a Probe of Mineral-Fluid Interfaces: A User Guide. *Reviews in Mineralogy and Geochemistry* **49**, 149-220.

Fenter, P., Catalano, J.G., Park, C., Zhang, Z., (2006) On the use of CCD area detectors for high-resolution specular X-ray reflectivity. *Journal of Synchrotron Radiation* **13**, 293-303.

Fenter, P., Lee, S.S., Park, C., Soderholm, L., Wilson, R.E., Schwindt, O., (2010) Interaction of muscovite (0 0 1) with Pu^{3+} bearing solutions at pH 3 through ex-situ observations. *Geochim. Cosmochim. Acta* **74**, 6984-6995.

Fenter, P.A., Park, C., Nagy, K.L., Sturchio, N.C., (2007) Resonant anomalous X-ray reflectivity as a probe of ion adsorption at solid–liquid interfaces. *Thin Solid Films* **515**, 5654-5659.

Gaucher, E., Robelin, C., Matray, J.M., Négrel, G., Gros, Y., Heitz, J.F., Vinsot, A., Rebours, H., Cassagnabère, A., Bouchet, A., (2004) ANDRA underground research laboratory: interpretation of the mineralogical and geochemical data acquired in the Callovian–Oxfordian formation by investigative drilling. *Physics and Chemistry of the Earth* **29**, 55-77.

Guo, Z., Niu, L., Tao, Z., (2005) Sorption of Th(IV) ions onto TiO_2: Effects of contact time, ionic strength, thorium concentration and phosphate. *Journal of Radioanalytical and Nuclear Chemistry* **266**, 333-338.

Harrowfield, J.M., Ogden, M.L., White, A.H., (1991) Actinide complexes of the calixarenes. Part 2. Synthesis and crystal structure of a novel thorium(IV) complex of p-tert-butylcalix[8]arene. *J. Chem. Soc. Dalton Trans.*, 2625-2632.

Hummel, W., Berner, U., Curti, E., Thoenen, T., Pearson, F.J., (2002) The NAGRA/PSI Chemical Thermodynamic Database 01/01. *Radiochimica Acta* **90**, 805-813.

Israelachvili, J., Wennerstrom, H., (1996) Role of hydration and water structure in biological and colloidal interactions. *Nature* **379**, 219-225.

Jakobsson, A.-M., (1999) Measurement and Modeling of Th Sorption onto TiO2. *Journal of Colloid and Interface Science* **220**, 367-373.

Johansson, G., (1968) On the structure of the hydrolysis products of thorium. *Acta Chem. Scand.* **22**, 399-409.

Knope, K.E., Wilson, R.E., Vasiliu, M., Dixon, D.A., Soderholm, L., (2011) Thorium(IV) molecular clusters with a hexanuclear Th core. *Inorg. Chem.* **50**, 9696-9704.

Landa, E.R., Le, A.H., Luck, R.L., Yeich, P.J., (1995) Sorption and coprecipitation of trace concentrations of thorium with various minerals under conditions simulating an acid uranium mill effluent environment. *Inorg. Chim. Acta* **229**, 247-252.

Lee, S.S., Fenter, P., Park, C., Sturchio, N.C., Nagy, K.L., (2010a) Hydrated Cation Speciation at the Muscovite (001)-Water Interface. *Langmuir* **26**, 16647-16651.

Lee, S.S., Nagy, K.L., Fenter, P., (2007) Distribution of barium and fulvic acid at the mica–solution interface using in-situ X-ray reflectivity. *Geochim. Cosmochim. Acta* **71**, 5763.

Lee, S.S., Nagy, K.L., Park, C., Fenter, P., (2009) Enhanced Uptake and Modified Distribution of Mercury(II) by Fulvic Acid on the Muscovite (001) Surface. *Environ. Sci. Technol.* **43**, 5295-5300.

Lee, S.S., Park, C., Fenter, P., Sturchio, N.C., Nagy, K.L., (2010b) Competitive adsorption of strontium and fulvic acid at the muscovite–solution interface observed with resonant anomalous X-ray reflectivity. *Geochim. Cosmochim. Acta* **74**, 1762-1776.

Li, W., Tao, Z., (2002) Comparative study on Th(IV) sorption on alumina and silica from aqueous solution. *Journal of Radioanalytical and Nuclear Chemistry* **254**, 187-192.

Marcus, Y., (1991) Thermodynamics of solvation of ions. Part 5.-Gibbs free energy of hydration at 298.15 K. *Journal of the Chemical Society, Faraday Transactions* **87**, 2995-2999.

Neck, V., Kim, J.I., (2001) Solubility and hydrolysis of tetravalent actinides. *Radiochimica Acta* **89**, 1-16.

Neck, V., Muller, R., Bouby, M., Altmaier, M., Rothe, J., Denecke, M.A., Kim, J.I., (2002) Solubility of amorphous Th(IV) hydroxide - application of LIBD to determine the solubility product and EXAFS for aqueous speciation. *Radiochimica Acta* **90**, 485-494.

Oelkers, E.H., Schott, J., Gauthier, J.-M., Herrero-Roncal, T., (2008) An experimental study of the dissolution mechanism and rates of muscovite. *Geochim. Cosmochim. Acta* **72**, 4948-4961.

Östhols, E., (1995) Thorium sorption on amorphous silica. *Geochim. Cosmochim. Acta* **59**, 1235-1249.

Östhols, E., Manceau, A., Farges, F., Charlet, L., (1997) Adsorption of Thorium on Amorphous Silica: An EXAFS Study. *Journal of Colloid and Interface Science* **194**, 10-21.

Park, C., Fenter, P., (2007) Phasing of Resonant Anomalous X-ray Reflectivity Spectra and Direct Fourier Synthesis of Element-Specific Partial Structures at Buried Interfaces. *Journal of Applied Crystallography* **40**, 290-301.

Park, C., Fenter, P.A., Nagy, K.L., Sturchio, N.C., (2006) Hydration and Distribution of Ions at the Mica-Water Interface. *Physical Review Letters* **97**, 016101.

Park, C., Fenter, P.A., Sturchio, N.C., Nagy, K.L., (2008) Thermodynamics, Interfacial Structure, and pH Hysteresis of Rb+ and Sr2+ Adsorption at the Muscovite (001)−Solution Interface. *Langmuir* **24**, 13993-14004.

Park, C., Fenter, P.A., Sturchio, N.C., Regalbuto, J.R., (2005) Probing Outer-Sphere Adsorption of Aqueous Metal Complexes at the Oxide-Water Interface with Resonant Anomalous X-Ray Reflectivity. *Physical Review Letters* **94**, 076104.

Parkhurst, D.L., Appelo, C.A.J., 1999. User's Guide to PHREEQC (Version 2) — A Computer Program for Speciation, Batch-Reaction, One-Dimensional Transport and Inverse Geochemical Calculations, Water-Resources Investigations Report 99-4259. U.S. Geological Survey, Denver, CO.

Pashley, R.M., (1981) DLVO and hydration forces between mica surfaces in Li+, Na+, K+, and Cs+ electrolyte solutions: A correlation of double-layer and hydration forces with surface cation exchange properties. *Journal of Colloid and Interface Science* **83**, 531-546.

Pashley, R.M., (1982) Hydration Forces between Mica Surfaces in Electrolyte-Solutions. *Adv. Colloid Interface Sci.* **16**, 57-62.

Pashley, R.M., Israelachvili, J.N., (1984) Dlvo and hydration forces between mica surfaces in Mg2+, Ca2+, Sr2+, and Ba2+ chloride solutions. *Journal of Colloid and Interface Science* **97**, 446-455.

Pearson, F.J., Arcos, D., Bath, A., Boisson, J.-Y., Fernández, A.M., Gäbler, H.-E., Gaucher, E., Gautschi, A., L. Griffault, Hernán, P., Waber, H.N., 2003. Mont Terri Project – Geochemistry of Water in the Opalinus Clay Formation at the Mont Terri Rock Laboratory.

Qian, L., Zhao, J., Hu, P., Geng, Y., Wu, W., (2010) Effect of pH, fulvic acid and temperature on sorption of Th(IV) on zirconium oxophosphate. *Journal of Radioanalytical and Nuclear Chemistry* **283**, 653-660.

Rand, M., Fuger, J., Neck, V., Grenthe, I., Rai, D., 2008. Chemical Thermodynamics of Thorium. North Holland Elsevier Science B.V., Amsterdam, The Netherlands.

Reiller, P., Casanova, F., Moulin, V.r., (2005) Influence of Addition Order and Contact Time on Thorium(IV) Retention by Hematite in the Presence of Humic Acids. *Environ. Sci. Technol.* **39**, 1641-1648.

Robinson, I.K., Tweet, D.J., (1992) Surface X-ray-Diffraction. *Rep. Prog. Phys.* **55**, 599-651.

Rojo, I., Seco, F., Rovira, M., Giménez, J., Cervantes, G., Martí, V., de Pablo, J., (2009) Thorium sorption onto magnetite and ferrihydrite in acidic conditions. *Journal of Nuclear Materials* **385**, 474-478.

Rothe, J., Denecke, M.A., Neck, V., MÃ¼ller, R., Kim, J.I., (2002) XAFS Investigation of the Structure of Aqueous Thorium(IV) Species, Colloids, and Solid Thorium(IV) Oxide/Hydroxide. *Inorg. Chem.* **41**, 249-258.

Ryan, J.L., Rai, D., (1987) Thorium(IV) hydrous oxide solubility. *Inorg. Chem.* **26**, 4140-4142.

Sakuma, H., Katsuyuki, K., (2011) Structure and dynamics of water on Li^+-, Na^+-, K^+-, Cs^+-, $H3O^+$-exchanged muscovite surfaces: A molecular dynamics study. *Geochim. Cosmochim. Acta* **75**, 63-81.

Schlegel, M.L., Nagy, K.L., Fenter, P., Cheng, L., Sturchio, N.C., Jacobsen, S.D., (2006) Cation sorption on the muscovite (0 0 1) surface in chloride solutions using high-resolution X-ray reflectivity. *Geochim. Cosmochim. Acta* **70**, 3549-3565.

Schmidt, M., Wilson, R.E., Lee, S.S., Soderholm, L., Fenter, P., (2012) Adsorption of Plutonium-Oxide Nanoparticles on Muscovite. *Langmuir* **28**, 2620-2627.

Sharma, P., Singh, G., Tomar, R., (2009) Synthesis and characterization of an analogue of heulandite: Sorption applications for thorium(IV), europium(III), samarium(II) and iron(III) recovery from aqueous waste. *Journal of Colloid and Interface Science* **332**, 298-308.

Sheng, G., Hu, J., Wang, X., (2008) Sorption properties of Th(IV) on the raw diatomite--Effects of contact time, pH, ionic strength and temperature. *Appl. Radiat. Isotopes* **66**, 1313-1320.

Soderholm, L., Almond, P.M., Skanthakumar, S., Wilson, R.E., Burns, P.C., (2008) The structure of the plutonium oxide nanocluster $[Pu_{38}O_{56}Cl_{54}(H_2O)_{(8)}]^{(14-)}$. *Angewandte Chemie-International Edition* **47**, 298-302.

Takao, S., Takao, K., Kraus, W., Emmerling, F., Scheinost, A.C., Bernhard, G., Hennig, C., (2009) First hexanuclear U^{IV} and Th^{IV} formate complexes – structure and stability range in solution. *Eur. J. Inorg. Chem.*, 4771-4775.

Talip, Z., Eral, M., Hiçsönmez, Ü., (2009) Adsorption of thorium from aqueous solutions by perlite. *Journal of Environmental Radioactivity* **100**, 139-143.

Walther, C., Fuss, M., Buchner, S., (2008) Formation and hydrolysis of polynuclear Th(IV) complexes - a nano-electrospray mass-spectrometry study. *Radiochimica Acta* **96**, 411-425.

Wickleder, M.S., Fourest, B., Dorhout, P.K., 2011. Thorium, in: Morss, L.R., Edelstein, N.M., Fuger, J., Katz, J.J. (Eds.), The Chemistry of the Actinide and Transactinide Elements, 4th ed. Springer, pp. 52-160.

Wilson, R.E., (2011) Structural periodicity in plutonium(IV) sulfates. *Inorg. Chem.* **50**, 5663-5670.

Wilson, R.E., Schwindt, O., Fenter, P., Soderholm, L., (2010) Exploitation of the sorptive properties of mica for the preparation of higher-resolution alpha-spectroscopy samples. *Radiochimica Acta* **98**, 431-436.

Wilson, R.E., Skanthakumar, S., Burns, P.C., Soderholm, L., (2007a) Structure of the homoleptic thorium(IV) aqua ion [Th(H2O)(10)]Br-4. *Angewandte Chemie-International Edition* **46**, 8043-8045.

Wilson, R.E., Skanthakumar, S., Sigmon, G., Burns, P.C., Soderholm, L., (2007b) Structures of dimeric hydrolysis products of thorium. *Inorg. Chem.* **46**, 2368-2372.

Zhang, H., Zheng, D., Tao, Z., (2006) Sorption of thorium(IV) ions on gibbsite: Effects of contact time, pH, ionic strength, concentration, phosphate and fulvic acid. *Colloids and Surfaces A: Physicochemical and Engineering Aspects* **278**, 46-52.